

Pre-impregnated Carbon Fibre Reinforced Composite System for Patch Repair of Steel I-beams

Allan Manalo, Chamila Sirimanna, Warna Karunasena, Lance McGarva, and Paul Falzon

1. Introduction

Many steel infrastructures around the world are structurally deficient and need retrofitting. Hollaway [1] defined a structurally deficient structure is one whose components may have deteriorated or have been damaged, resulting in restrictions on its use. In steel structures, the deterioration may be due to corrosion, impact damage, and/or fatigue cracking due to the increase in traffic density, environmental attack and lack of proper maintenance [2]. A common approach of retrofitting structurally deficient steel structures is welding or bolting new steel material onto degraded structures [3]. In the case of the offshore industry, the total cost of a welding repair can be dramatically increased because of the need to shut down production during “hot works” for safety reasons. Hence there is a strong incentive to introduce improved repair approaches, such as adhesively bonded composite repairs, that avoid the need for hot work conditions.

Adhesively bonded repairs have been used for several decades in the defence industry for the maintenance and life extension of aircraft, both made from metal and composites [4]. In recent decades, the application of fibre-reinforced polymer (FRP) composites for strengthening and rehabilitation of structural elements has become essential [2]. Hollaway [1] reported that adhesively bonded FRPs have been used extensively to strengthen concrete structures due to their high strength-to-weight ratio and excellent corrosion resistance. FRP composite repairs offer other advantages: they can be shaped to almost any substrate geometry, they can be optimised and designed to avoid introducing unwanted load paths by using the anisotropy of the composite material, and they can be very lightweight, thus avoiding the need for heavy lifting equipment during repairs. Moreover, using composites

in rehabilitation does not require closing of the bridge to traffic [5]. These advantages present great opportunities for the utilisation of FRP composites for strengthening and rehabilitating of steel structures.

A number of researchers have now established the effectiveness of using bonded carbon fibre reinforced polymer (CFRP) for rehabilitating steel structures [1-2, 6-8]. However, most of the research and developments focused on using CFRP strips or plates in strengthening metallic structures. In most cases, the damage due to corrosion or fatigue cracks are localised in a beam. Similarly, the use of CFRP strips and plates are limited to flat steel surfaces. There is a need therefore to investigate the potential of a more flexible CFRP system to repair the damage allowing its application to steel structures of various shapes and sizes.

Teng et al. [9] indicated that FRP laminates formed via wet lay-up process are applicable to curved and irregular steel surfaces. Accordingly, Ekiz and El-Tawil [10] used CFRP wraps to improve the buckling and post-buckling response of steel plates. Similarly, Zhang et al. [11] proposed an innovative method involving impregnation of composites for steel railway bridges. In their study, the CFRP repair was cured on site under vacuum assisted pressure. While pre-impregnated composites has been applied for the restoration of an historic building, Hollaway [1] reported that only a few investigations used this type of composite repair systems to upgrade steel structures and further studies on their effectiveness in strengthening and/or rehabilitating structurally deficient steel structures are warranted.

To simulate the actual damage in steel structures, several researchers intentionally created notches of different sizes and geometries. For example, Al-Saidy et al. [6] and Kim and Harries [12] investigated the static and fatigue performance CFRP repaired beams with intentionally created damages at the tension flange of the beam. Similarly, Photiou et al. [13] investigated the behaviour of artificially degraded steel beam strengthened with carbon/glass

composite system. The damage to the beam was induced by removing (corrosion) or cutting (crack) part of the tension flange. Zhao and Zhang [8] and Kamruzzaman et al. [2] mentioned that these simulated defects should closely replicate the actual damage in the structure. Equally important is the determination of the effective bond length for CFRP laminates adhered to the steel to effectively utilise the composite material beam [5].

In this study, the effectiveness of a new type of carbon fibre reinforced epoxy repair system is evaluated as a potential patch repair system for retrofitting structurally deficient steel structures. Preliminary investigation conducted by Falzon et al. [14] has successfully demonstrated that this new material system can fully restore the pressure capacity of corroded steel pipelines. The shape flexibility of this new type of composite repair system makes it an attractive material in strengthening and rehabilitating of structures. Moreover, this advanced processing technique can potentially improve the curing process, bond strength and speed of application compared to CFRP plate and wet lay-up systems where curing of resins takes up to several days under ambient conditions to achieve full load capacity. This study further examines the potential application of this system in the rehabilitation of steel I-beams with simulated defect on the tension flange under static flexural load. The assessment of the carbon fibre prepreg system through mechanical testing of tensile and double strap shear joint specimens is also included.

2. Carbon prepreg system

The development of the carbon prepreg system for composite repairs is driven by the need to match the stiffness of early and model steel structures. As glass fibre composite has a significantly lower Young's Modulus than steel, it can result in repairs that are significantly thicker than the steel substrate, which may be time consuming to apply or there may be insufficient room for the repair itself. Consequently, there are significant benefits that can be realised by using a reinforcement of greater Young's modulus, such as carbon fibre.

Although the fibre itself is more expensive, the reduced amount of material required and the shorter application time provide opportunity to significantly reduce the overall cost of the repair. Moreover, DNV-RP-C301 [15] mentioned that using pre-impregnated reinforcement layers eliminate the need to handle resins during repair and ensures a better control over impregnation process and the fibre-resin ratio resulting in a more uniform quality of repair.

The MTT989C prepreg system [14] used in this study is based on a non-crimp carbon fibre reinforcement constructed using 50k Panex 35 carbon fibre with 400 gsm unidirectional layers in the 0° (longitudinal) and 90° (transverse) directions, giving an areal weight of 815 gsm. The specific weight was chosen as it would allow adequate wet-out during the impregnation process. The bi-directional non-crimp fabric reinforcement, supplied in 300 mm wide rolls, was converted into a prepreg system by Specialty Coatings. The impregnation was performed using a wet resin bath process, where the resin content was accurately controlled. The resin used was an epoxy based system which is identical to that used in PETRONAS ProAssure™ Wrap Extreme glass fibre repair material system for onshore and offshore pipeline. The resulting prepreg had an areal weight of 1765 gsm and fibre volume fraction of 65%. Each ply, in its cured state, has a thickness of approximately 1 mm.

3. Experimental program

A large testing program consisting of tensile test of coupons, double strap shear joint tests and flexural tests of steel I-beams were conducted in order to assess the structural performance of the new carbon/epoxy prepreg system.

3.1 Test matrix

The specimen preparation and test procedures were based on ISO/TS 24817 [16] and DNV-RP-C301 [15]. Tests included longitudinal and transverse tensile tests of the carbon/epoxy prepreg system produced by vacuum and low-pressure consolidation, double strap shear

joint tests, and four-point bending tests of patch repaired steel I-beams. In addition, an undamaged steel I-beam was tested as a control beam. All tests were performed at room temperature and where possible, the results were compared to equivalent tests performed on glass/epoxy specimens, previously reported [17].

3.2 Specimen preparation

The procedures used to manufacture the specimens are described below.

3.2.1 Surface Preparation

Gholami et al. [3] indicated that appropriate preparation of the steel surface where the FRP repair will be applied is an important step governing the quality of adhesive bonded joint. Consequently, the steel substrates of all specimens in this study were prepared to a surface roughness of 50-60 μm by grit blasting using Garnet 16/40 grit. Measurements were performed using Testex tape according to ASTM D4417 [18]. Bio-Fix 911 epoxy filler was used to fill the simulated defects in the beam specimens prior to application of primer and carbon patch repairs.

3.2.2 Cure conditions

Two different methods were used to consolidate the prepreg during manufacture of specimens as shown in Figure 1a. Tension specimens were consolidated either with vacuum at 0.92 bar (92 kPa) or with the application of external weights applying a low consolidation pressure of 2 kPa using a 26 mm thick steel plate with dimensions 300 x 300 mm. The double strap shear specimens and patch-repaired beams were consolidated using vacuum (Figure 1b). In applying the CFRP repair, each ply is consolidated using a 80 mm x 20 mm diameter fin roller to ensure that the layers are in contact with each other. After applying the required number of layers, the laminate is covered with a WL5200B release film. A breather ply is then placed over a release film to prevent resin leaking from the lay-up. The vacuum bagging film is then placed over the breather ply, sealed with tacky tape and the vacuum is then

applied. All specimens including the steel I-beams were cured in an oven at 55°C for 48 hours.

3.2.3 Tension specimens

Longitudinal tension (LT) and transverse tension (TT) coupons were manufactured for testing in accordance with ASTM D3039 [19]. Five replicates each in the LT and TT coupons consolidated by vacuum, and LT coupons produced using low consolidation pressure were tested. The nominal dimensions and details of the tension specimens are shown in Figure 2. Tabs were used at both ends to keep the specimens from end-crushing. The LT specimen lay-up was $[0/90]_{2s}$ and the TT specimen lay-up was $[90/0]_{2s}$.

3.2.4 Double strap shear specimens

Teng et al. [9] indicated that, in most cases, the interfacial debonding failures control the load-carrying capacity of steel structures strengthened with fibre composites. This bond behaviour between the substrate and the bonded FRP materials is commonly studied through pull-out test. Thus, double strap shear specimens were prepared and tested to determine the effective bond length for the prepreg CFRP repair system. Zhao and Zhang [8] indicated that a double strap shear test is most suitable for steel I-beam strengthened with CFRP as it closely replicates the adhesive shear and peel stress induced by flexural loads on the beam at the pure bending zone. Haghani and Al-Emrani [20] further indicated that a double-sided strengthened steel plate is less sensitive to the thickness of the steel plate than a single-lap joint, and therefore adopted in this study.

A total of 20 specimens were tested to determine the effective bond length for the prepreg CFRP repair. The double strap shear joints were manufactured in accordance with DNV-RP-C301 Appendix I [15] and were comprised of two 5 mm thick BlueScope Steel Xlerplate adherends, spaced 5 mm apart, bonded together with PR25 primer and prepreg

CFRP patches on both sides. PR25 is part of the current ProAssure™ Wrap Extreme material system and is applied at a thickness of 1150 gsm. BlueScope Steel Xlerplate was chosen because it complies with ASTM A36 [4]. Four different overlap lengths, l of 25 mm, 50 mm, 75 mm and 120 mm were created by machining slots through the laminate on one end of the joint, top and bottom, as shown in Figure 3. On the other hand, a longer bond length (150 mm) was provided on one end to ensure that debonding will happen in the overlap length. The laminate lay-up was $[0/90]_{3S}$ and specimens were cured under vacuum.

3.2.5 *Beam specimens*

Carbon patch repairs were applied to two steel I-beams that contain simulated damage. The purpose of the tests was to investigate the suitability of the carbon prepreg system to restore the integrity of steel structures. The 150UB14 Orrcon Steel (14 kg/m) steel I-beams were manufactured to AS/NZS3679.1 [21] and has a similar composition to the steel plate used for the double strap shear specimens. As reported by Yu et al. [22], the Young's modulus, yield strength and ultimate strength of this beam is around 192 GPa, 334 MPa and 483 MPa, respectively. The dimensions of the 150 UB14 steel I-beams are provided in Figure 4. This section is considered as a shallow beam (overall depth to flange width ratio of 2.0) as suggested by Nakashima et al. [23] for a stable beam section.

The damage consisted of a simulated crack and 80% corrosion defects, located at mid span, in the tension flange of the beam (Figure 4). The crack is simulated using a 1 mm wide rectangular notch through the whole flange width. On the other hand, the corrosion damage is induced by machining and removing 80% of the total thickness of the tension flange (from 7 mm to 1.4 mm) for a length of 90 mm. The end of the corrosion defect was then tapered in 45° to minimise any stress concentration. The simulated defects were filled with Bio-Fix 911 filled epoxy grout prior to repair application. Steel stiffeners (5 mm thick) were

welded on both sides of the web at the loading and supporting points to prevent premature flange buckling and web crushing.

The carbon patch repairs were sized to match the stiffness of the steel removed from the tension flange of the beams. Appendix A shows the calculation of the required thickness of the prepreg carbon patch for each beam. A total of 15 plies were used for the crack-patched beam and 11 plies for the 80% corroded beam. A layer of 47 gsm glass tissue was placed between the carbon repair wrap and steel beam to prevent galvanic corrosion. Repair plies were wrapped around the flange and half way up the web of the beam, incorporating an edge taper of approximately 50 mm, as shown in Figures 5 and 6. Deng and Lee [7] and Haghani and Al-Emrani [20] indicated that tapering of the laminates can be employed to reduce the interfacial stress concentration at the ends of the composite repair and to prevent debonding failure. The tapered ends were implemented by using different length of prepreg laminates.

3.3 Experimental set-up and procedure

The tension specimens were loaded at a displacement rate of 2 mm/min and strains recorded using a biaxial extensometer. The failure stress and Young's modulus were calculated from the tests using procedures outlined in ASTM D3039 [19]. On the other hand, tensile testing of steel-carbon double strap shear joints was undertaken to characterise the debonding that originates from a crack covered by a CFRP patch. The double strap shear joints were tested in accordance with DNV-RP-C301 Appendix I [15]. The test setup is shown in Figure 7. During the tests, specimens were loaded at a rate of 0.5 mm/min. Laser displacement transducer was used to measure the relative displacement between the steel plates.

The 3.0 m long steel I-beams were statically loaded under four-point-bending, supported at positions 300 mm from each end and loaded at a span of 800 mm, through a steel spreader beam, as shown in Figure 8. Uni-axial strain gauges were attached on the top and bottom flanges of the beam, as shown in Figure 9, to measure the longitudinal strain during loading.

A laser displacement transducer was used to measure the centre span deflection of the beam. The load was applied by a 200 kN hydraulic jack at a rate of 3 mm/min until yielding of the steel I-beam was observed. All data, including the load values measured by a load cell, were recorded by the System5000 data logging system. The tests were stopped when a significant decrease in test load was detected or significant deformation or lateral buckling was observed.

4. Results and discussion

The results of the experimental evaluation of repair system performance and relevant discussions are presented in the following sections.

4.1 Tensile behaviour of carbon prepreg system

The results of the tensile tests of coupons are given in Table 1. The tensile strength and modulus are calculated based on the actual thickness of the laminate. The use of vacuum during laminate manufacture resulted in a slight improvement in Young's modulus and a small improvement in tensile strength of around 5%. This improvement is due to the better consolidation of the fibre layers due to vacuum as indicated in the microscopic observation through the cross-section of the laminates as shown in Figure 10. Hollaway [1] indicated that prepreg composites would give a high strength compacted repair systems. As can be seen in Figure 10c, some layers in the laminate produced with no vacuum are not bonded properly to each other. Although the carbon reinforcement is balanced, with equal quantity of fibres in the longitudinal and transverse direction, the transverse tensile properties were slightly lower than the longitudinal properties. This difference is likely due to variation in the fabric, particularly fibre waviness, introduced during the fabric and/or prepreg manufacturing processes. All of the tested specimens failed with large amounts of fibre breakage and delamination, as shown in Figure 11. The tensile modulus and strength of the carbon system was approximately 300% and 270% of the modulus and strength of the

glass/epoxy ProAssure™ Wrap Extreme system, respectively. The glass/epoxy values were obtained from the qualification testing program [17]. The significantly higher mechanical properties allows for the design and application of carbon repairs that are three times thinner than repairs using the glass system.

4.2 Behaviour of double strap shear joint

The typical plots of load against cross-head displacement are shown in Figure 12. The figure shows that with shorter overlap lengths of 25 mm and 50 mm, the load increases linearly until the joints fail completely. However, with longer overlap lengths of 75 mm and 120 mm, the load increases linearly until stable crack propagation initiates. As the test continues (in displacement control), the crack or disbond grows at constant load until the remaining bond becomes too small to withstand the applied load, and complete failure occurs.

The average failure load per unit width (and standard deviation) for each overlap length of the double strap shear specimens was calculated and is given in Table 2. In this calculation, the adhesive shear stress is assumed to be constant along the bond length as well as the through thickness of the adhesive layer. The failure load, or patch force, per unit width f as a function of overlap length L , for each test specimen, is plotted in Figure 13. This f - L curve shows that the fracture force is proportional to the overlap length for short overlaps and for long overlap lengths it reaches a plateau level where the fracture load is independent of overlap length.

Teng et al. [9] indicated that the bond strength is the ultimate tensile force that can be resisted by the composite repair before debonding failure occur. Moreover, this bond strength increases with bond length but when it reaches a threshold value, any further increase in the bond length does not lead to an increase in the bond strength. Nozaka et al. [5] further indicated that the effective bond length is the bond length that produces the maximum possible stress or the shortest bond length that maximises the load transferred into

the CFRP repair. Based on the experimental results, the critical plastic shear stress τ_p of the bondline was estimated from the initial slope of the f - L curve. The minimum overlap length of a patch repair should be long enough to ensure that a significant region of the bondline between the centre and edges of the patch are unloaded. This is normally achieved if the overlap length is

$$L > 2F/w \tau_p$$

where F is the patch load at fracture and w is the width of the patch. Shorter maximum overlap may be accepted if it can be shown that the minimum shear stress in the bondline at fracture does not exceed 10% of the critical plastic shear stress [15]. For the patch thickness and configuration tested, the minimum overlap length for a patch repair is calculated as approximately 60 mm. Consequently, there will be no further increase in the bond strength at a length above 60 mm, indicating that this is the effective bond length for the prepreg CFRP. However, a bond length of 120 mm is selected and adopted in the preparation of the beam as this provides a more consistent and reliable bond strength. The coefficient of variation achieved for this bond length is only around 0.5%. Moreover, this bond length is considered practical as Yu et al. [22] indicated that the development length for FRP strips bonded with epoxy is normally around 200 mm. The maximum bond strength attained for the 120 mm bond length is around 740 N/mm width.

Photographs of failed double strap shear joint specimens are shown in Figure 14. It was found that the specimens with short bond length failed by cohesion failure, where fracture of the epoxy adhesives was observed near the end of the joint. This is because of the high shear stress concentration at the end of the bondline which explains the high variation of the measured patch load up to a bond length of 75 mm as shown in Figure 13. When the bond length was increased to 120 mm, the joint failed by the steel and adhesive interface debonding failure indicating a stronger bond capacity of the adhesives to the FRP than that

of the steel. The uniform stress distribution along the bondline explains the more consistent patch load obtained for 120 mm than the shorter bond lengths. Teng et al. [9] indicated that the adhesion failure between the steel and the adhesive is much more likely to happen for steel with externally bonded FRP reinforcement due to the difficulty in the surface preparation of steel. Thus, it is anticipated that this failure behaviour will replicate the failure behaviour of strengthened tension flange of the steel I-beam.

4.3 Behaviour of patch repaired steel I-beams

Table 3 summarises the results of the three structural beam tests. The results indicated that the composite patch repairs were effective at restoring the original load carrying capacity of the damaged beams to that of an undamaged beam. The maximum load carried by the repaired beam with a cracked flange and 80% corrosion was 3% and 8% higher load than the maximum load carried by the undamaged beam, respectively. During the tests, all of the beams exhibited yielding of the steel, followed by lateral instability.

The load and mid-span deflection relationship curve of the undamaged steel I-beam and repaired beams are shown in Figure 15. In the plot, the specimen I-beam, 80% and crack correspond to the steel I-beam without defect, beam with simulated 80% corrosion defect and beam with crack, respectively. All the beams exhibited almost linear elastic behaviour up to an applied load of 90 kN, after which a nonlinear load deflection was observed. Both the repaired beams showed a very similar behaviour and exhibited 16% higher global bending stiffness compared to the undamaged beam. However, there was no plastic hinge observed for these beams. Although the repair patches were sized for stiffness, there is a considerable amount of repair material outside of the damaged regions of the flange and on the web of the beams and it was not unexpected that the repaired beams would exhibit slightly greater stiffness than the undamaged beam. The measured stiffness of the repaired beams is 6.4 kN/mm compared to 5.5 kN/mm for the undamaged beam. This could be

probably due to the increase in the total depth of the repaired beam as the patched composite repair was bonded to the bottom of the tension flange resulting in the increase in the overall second moment of area of the section.

Load-deflection curves started showing non-linear behaviour for all beam specimens at an applied load of approximately 90 kN, indicating that the yielding of the steel beam occurred. At this load, the stress in the top and bottom surfaces of the flanges can be calculated as 405 MPa ($I_{xx} = 6.66 \times 10^6 \text{ mm}^4$). The test certificate provided by the manufacturer of the steel beams gives the average yield strength of the steel as 368 MPa. This is supported by the strain measurements from the uni-axial strain gauges attached to the undamaged beam. Strain measured at the topmost (strain gauge 6) and bottommost (strain gauge 1) surfaces of the flange, shown in Figure 16, increased linearly up to a strain of approximately 1860 microstrains, indicating a stress of 372 MPa. For beams with composite patch repair, the yielding of the steel is slightly delayed. As indicated in the load-strain curve, the repaired beams started to yield at an applied load of around 94 kN compared to 90 kN for undamaged steel I-beam, which is 4% higher.

Similar behaviour was recorded by strain gauges attached to the repaired beams. Strains in all the 6 gauges generally increased linearly with the applied load until yielding of the steel beam, shown in Figures 17 and 18. Refer to Figures 8 and 9 for the locations of the attached strain gauges. Nonlinear behaviour was then observed, particularly at the strain gauges attached directly to the steel (4 and 6). It is important to note that yielding occurs firstly in the tension flange outside the section with patch repair as shown by the nonlinear stress-strain behaviour of the gauge no. 4 or the strain gauge attached 20 mm from the end of the composite patch repair. The response of the strain gauges in this location is linear up to a load level of around 77 kN or strain of 1600 microstrains. Thereafter, the beam continued to carry load until the compressive buckling of the compressive flange. Once the

compression flange yields, no further load is taken by the beam and it undergoes plastic deformation. The load then dropped owing to final failure in the beam. It was observed that the beam behaviour is controlled by the local buckling of the compression flange followed by lateral buckling of the beam. Further, Teng et al. [9] indicated that buckling failure becomes more critical after the tension flange is strengthened with FRP as the compression flange needs to sustain a higher load level before the beam fails. Thus, this type of failure is anticipated as there is no sufficient lateral restraint along the length of the beam.

Up to the yielding of the steel, the patch repair remained fully bonded to the steel indicating generally sound bond quality of the composite repair. This suggests that the objective of restoring the capacity and stiffness of the defected beams using carbon patch repair systems under flexural loading is successfully achieved. This also suggests that the patch repair was applied with sufficient bond length to prevent any debonding failure on or before the steel yields. These observations clearly demonstrate the effectiveness of the prepreg CFRP system in repairing steel I-beams. Previous studies highlighted that this level of efficiency for CFRP plates [6, 7] and laminates [9, 20] can only be achieved when an equivalent longitudinal stiffness (EA) of repair system is used to replace the area of steel with defects and when no debonding occurs between the steel and the repair system up to yielding of the steel. Upon continuation of the application of the load, the patch repair to the beam with the 80% corrosion defect failed by debonding at the end of the patch but most part of it remained attached to the beam, as shown in Figure 19. On the other hand, there was no debonding failure observed in the repaired beam with simulated crack defect. This is an interesting result as the overall length of the patch repair for the beams with 80% corrosion defect is longer and the end of the is closer to the support than that of the repaired beam with simulated crack defect. This can be due to the local yielding on the machined and reduced section of the beam.

The debonding failure at the end of the patch repair can also be explained by the strain incompatibility of the repaired and unrepaired sections of the beam. Figure 20 shows the strain distribution along the length of the patch repair (gauges 1, 2 and 3) as well as on the steel outside the repair (gauge 4) at various levels of applied load. As can be seen from the figure, the strain level in all gauges is almost same up to the 60 kN. This is expected as all these strain gauges are attached within the location of the constant moment region and experienced almost the same level of stress. Moreover, the beam is still in the linear elastic region. After the steel yielded at an applied load of 80 kN, the strain in gauge 4 increased rapidly due to its plasticity but the strain reading near the end of the patch repair (gauge 3) dropped, which may indicate the onset of epoxy debonding. However, since the test was stopped due to lateral buckling of the beam, the debonding failure was not realised.

The microscopic observations in Figure 21 showed that the beam with 80% corrosion has an almost double thicker gluelines than that of the repaired beam with crack. Yu et al. [22] and Osnes and McGeorge [24] suggested that the bond strength increases when the thickness of the adhesive decreased. They further mentioned that thicker bondlines may contain more defects such as voids and microcracks. As a result, composite patch repair with a thicker bondline may fail at lower load than the thinner bondlines. There are also signs of delamination near the end of the machined section for repaired beam with simulated 80% corrosion defect. This may explain why the repaired beam with 80% corrosion defect failed due to debonding but the beam with a crack defect did not. On the other hand, lateral buckling occurred at a lower load for repaired beam with a crack defect than the beam with 80% corrosion defect. This showed that the stability of the repaired beam with 80% corrosion damage is higher than the beam with a crack defect. This is due to the longer CFRP patch attached to the tension flange with 80% simulated defect. Yu et al. [22] further indicated that beams with longer FRP laminate will result in a larger effective tension area of the beam and

will lead to a higher failure load, which explains the earlier occurrence of the lateral buckling in repaired beam with crack compared to that of the repaired beam with 80% corrosion defect.

5. Evaluation of patch repair thickness for different levels of defect

Teng et al. [9] indicated that the in-plane bending stiffness of a repaired I-beam can be easily determined provided that debonding does not become critical and hence the plane section assumption can be used. Following this assumption and the calculation method presented in Appendix A, a parametric study was implemented to evaluate the required thickness of a patch repair system to restore the flexural stiffness of steel I-beams with 20 to 100% defect on the tension flange. Three different patch repair systems with different Young's modulus were considered including the prepreg CFRP [0/90] and GFRP systems with properties listed in Table 2 as well as unidirectional prepreg CFRP [0] (Young's modulus = 90.5 GPa). Here, the patch repair was applied with sufficient bond length to prevent any debonding failure on or before the steel yields. The results of this analysis is presented in Figure 22.

It can be seen clearly from the figure that the required thickness of repair increases with increasing level of defects. For example, from 2.2 mm thick prepreg CFRP [0/90] needed to restore the flexural stiffness of a steel I-beam with 20% defect, this requirement increases to 10.9 mm thick when the full thickness of the tensile flange has a defect. As expected, the prepreg GFRP requires the thickest repair system due to its relatively lower Young's modulus compared to CFRP [0/90]. Based on the analysis, at least 3 times more GFRP is required to repair the same level of defect compared when CFRP [0/90] is used. Consequently, this repair system will require 3 times longer time to lay all the laminates and will be 5 times heavier than CFRP. The results also showed that the prepreg CFRP [0] requires the least amount of fibres to restore the stiffness of the steel I-beams as this repair system has the highest Young's modulus among the repair systems considered.

6. Conclusion

The performance of carbon fibre reinforcement pre-impregnated with epoxy resin as a patch repair systems for steel structures has been investigated through tensile tests, double strap shear tests, and structurally rehabilitated steel beam. Based on the results of the study, the following conclusion can be drawn:

- The tensile modulus and strength of the pre-impregnated carbon fibre reinforced composite system is approximately 300% and 270%, respectively than that of similar glass/epoxy composite repair system. This allows a considerable reduction in the size of repairs and consequently a reduction in the repair application time.
- The use of vacuum during laminate manufacture results in better mechanical properties for carbon prepreg system. The tensile modulus and strength is around 5% higher than that of the specimens prepared without vacuum due to the better consolidation of the fibre layers.
- The effective bond length of carbon prepreg system is found to be around 60 mm but a bond length of 120 mm provides a more consistent and reliable bond strength. The failure mode of double lap shear joints was interfacial failure at the steel-adhesive interface.
- The characteristic strength of the double strap shear joint is representative of the bond strength of the rehabilitated steel beam. No debonding failure was observed in the repaired steel I-beam up to the yielding of the steel, suggesting that the carbon patch repair is bonded adequately to the flanges.
- The patched carbon prepreg system successfully demonstrated the ability to repair crack and corrosion defects in steel I-beams, restoring them to their original load carrying capacity and stiffness. Both repaired beams exhibited 16% higher stiffness and failed at an applied load of at least 3% higher than the undamaged beam.

Moreover, the provision of the composite repair slightly delayed the yielding of the steel.

- The thickness of the epoxy adhesives and length of repair were found to affect the overall behaviour of the repaired I-beams. The patch repair with a thicker bondline is more prone to debonding failure while a longer patch repair results in a more stable beam compared to that of the beam with thinner bondline and shorter patch repair, respectively.

While the flexible prepreg carbon repair system is found suitable for curved steel surface, the bi-directional form of the prepreg material that was evaluated may not be the most effective form for rehabilitation of structural members loaded in bending, where the fibres in the transverse direction contribute little to the stiffness or strength of the repair patch. It is recommended that a unidirectional carbon prepreg repair system should be developed and its potential for rehabilitating steel structures should be investigated.

Acknowledgements

This work was undertaken as part of a CRC-ACS research program, established and supported under the Australian Government's Cooperative Research Centres Program.

References

- [1] Hollaway, L.C., Advanced fibre polymer composite structural systems used in bridge engineering, ICE Manual of Bridge Engineering, 503-529, 2008.
- [2] Kamruzzaman, M., Jumaat, M.Z., Sulong, N.H.R., and Islam, A.B.M.S., A review on strengthening steel beams using FRP under fatigue, The Scientific World Journal, 1-21, 2014.
- [3] Gholami, M., Sam, A.R.M., Yatim, J.M., and Tahir, M.M., A review of steel/CFRP strengthening systems focusing environmental performance, Construction and Building Materials, 47: 301-310, 2013.

- [4] Karbhari, V.M. and Seible, F., Fiber reinforced composites – Advanced materials for the renewal of civil infrastructure, *Applied Composite Materials*, 7: 95-124, 2000.
- [5] Nozaka, K., Shield, C.K. and Hajjar, J.F., Effective bond length of carbon-fibre-reinforced polymer strips bonded to fatigued steel bridge I-girders, *ASCE Journal of Bridge Engineering*, 10(2): 195-205, 2005.
- [6] Al-Saidy, A.H., Klaiber, F.W. and Wipf, T.J., Repair of steel composite beams with carbon fiber-reinforced polymer plates, *ASCE Journal of Composites for Construction*, 8(2): 163-172, 2004.
- [7] Deng, J. and Lee, M.M.K., Behaviour under static loading of metallic beams reinforced with a bonded CFRP plate, *Composite Structures*, 78: 232-242, 2007.
- [8] Zhao, X.L., Zhang, L., State-of-the-art review on FRP strengthened steel structures, *Engineering Structures*, 29: 1808-1823, 2007.
- [9] Teng, J.G., Yu, T. and Fernando, D. Strengthening of steel structures with fiber-reinforced polymer composites, *Journal of Constructional Steel Research*, 78: 131-143, 2012.
- [10] Ekiz, E. and El-Tawil, S., Inhibiting steel brace buckling using CFRP wraps, Proc. 8th USQ National Conference on Earthquake Engineering, San Francisco, California, USA, 2006.
- [11] Zhang, L., Hollaway, L., Teng, J. and Zhang, S., Strengthening of steel bridges under low frequency vibrations, *Proceedings of Composites in Civil Engineering (CICE 2006)*, Miami, Florida, USA, 2006.
- [12] Kim, Y.J., Harries, K.A., Fatigue behaviour of damaged steel beams repaired with CFRP strips, *Engineering Structures*, 33(5): 1491-1502, 2011.

- [13] Photiou, N.K., Hollaway, L.C., Chryssanthopoulos, M.K., Strengthening of an artificially degraded beam utilising carbon/glass composite system, *Construction and Building Materials*, 20: 11-21, 2006.
- [14] Falzon, P.J., Leong, K.H., McGarva, L., Leong, Y.L., Manalo, A., Virk, A., Leipnik, D., Djukic, L.P., Development and assessment of a carbon fibre reinforced composite repair system, 8th Asian-Australasian Conference on Composite Materials, 6-8 November 2012, Kuala Lumpur, Malaysia.
- [15] DNV-RP-C301. Design, Fabrication, Operation and Qualification of Bonded Repair of Steel Structures. Det Norske Veritas. 04/01/2012.
- [16] ISO/TS 24817 – Petroleum, petrochemical and natural gas industries – Composite repairs for pipework – Qualification and design, installation, testing and inspection (International Organisation for Standardization, 2006)
- [17] Djukic, L.P., Falzon, P.J., Leong, K.H., Leong, Y.L., Qualification of a Composite System for Oil and Gas Pipeline Repairs Part 1: Mechanical Properties, 8th Asian-Australasian Conference on Composite Materials, 6-8 November 2012, Kuala Lumpur, Malaysia, Paper O-REP-352.
- [18] ASTM D4417-03 – Standard test methods for field measurement of surface profile of blast cleaned steel. ASTM International, West Conshohocken, Philadelphia, Pa 19103.
- [19] ASTM D3039-08 – Standard test method for tensile properties of polymer matrix composite materials. ASTM International, West Conshohocken, Philadelphia, Pa 19103.
- [20] Haghani, R., Al-Emrani, M., A new design model for adhesive joints used to bond FRP laminates to steel beams – Part A: Background and theory, *Construction and Building Materials*, 34: 486-493, 2012.

- [21] ASTM A3679.1-2010 – Structural steel, Part 1: Hot-rolled bars and sections. ASTM International, West Conshohocken, Philadelphia, Pa 19103.
- [22] Yu, Y., Chiew, S.P. and Lee, C.K. Bond failure of steel beams strengthened with FRP laminates – Part 2: Verification, *Composites: Part B*, 42: 1122-1134, 2011.
- [23] Nakashima, M., Liu, D. and Kanao, I., Lateral-torsional and local instability of steel beams subjected to large cyclic loading, *International Journal of Steel Structures*, 3(3): 179-189, 2003.
- [24] Osnes, H., McGeorge, D., Experimental and analytical strength analysis of double lap joints for marine applications, *Composites: Part B*, 40: 29-40, 2009.

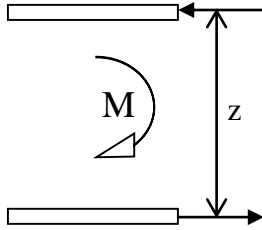
Appendix A. Calculation of the thickness of composite repair for beams with simulated defect

The design of structures with fibre composites are mostly govern by stiffness rather than strength, the defected portion of the steel I-beam is replaced with an equivalent area of CFRP patch to keep the overall bending stiffness of the beam unchanged. Similarly, the DNV-RP-C301 [15] strongly recommended designing the patch repair with strength in excess of the demands such that the failure of the patch itself is avoided.

In an I-beam, the bending stresses are assumed to be normally carried by the top and bottom flanges with the web resisting the shear. This assumption was considered in the preliminary calculation of the required thickness of composite patch repair to replace the ineffective layer of the tension flange due to corrosion and/or crack defects. Further, a full composite action and the patch repair is subjected to constant axial stress were assumed.

A.1 For I-beam with simulated crack defect in the tension flange

The required thickness of the carbon prepreg system to replace the crack defect in the flange of the steel I-beam is calculated as shown below:



$$C = A_f \sigma_y = (7)(75)(334) = 175.35 \text{ kN}$$

$$M = Tz = Cz = (175.35 \text{ kN})(143 \text{ mm}) = 25.08 \text{ kN-m}$$

$$T = A_f \sigma_y = (7)(75)(334) = 175.35 \text{ kN}$$

where C and T are the forces resisted by the compression and tension flanges, respectively, A_f is the area of the flange, σ_y is the yielding strength of the steel, M is the moment capacity, and z is the distance from the centroid between the top and bottom flanges.

Based on the 4-point static bending test set-up, the estimated applied load, P when the steel yields is around 62.69 kN ($P = 2M/0.8\text{m}$). Similarly, the strain in the steel at yielding is around 0.00174 (334 MPa/192,000 MPa) and the corresponding stress in prepreg CFRP when the steel yields is 92 MPa (52.9 GPa x 0.00174). Consequently, the required area of prepreg CFRP is 1906 mm² (175.35 kN/92 MPa). Assuming that the width of prepreg CFRP that will cover the bottom and top surfaces of the tension flange is 145 mm, then the required thickness of the CFRP patch repair is around 13.15 mm or 15 layers.

A.2 For I-beam with 80% corrosion on the tension flange

The capacity of the uncorroded portion of the beam is around 35.07 kN (0.20*175.35 kN) and the required axial force to be carried by patch repair is 140.28 kN (175.35 – 35.07 kN). This equates to a required area of prepreg CFRP of 1525 mm² (140.28 kN/92 MPa) or a thickness of 10.51 mm (1525 mm²/145 mm). Thus, a total of 11 layers of prepreg carbon system are required to replace the simulated 80% corrosion damage on the tension flange of the beam.

Table 1: Average modulus and failure load of coupons (Std. Dev. in parentheses)

Type	Property	Carbon		Glass
		Vacuum	No Vacuum	No Vacuum
LT	Modulus (GPa)	52.9 (5.6)	51.1 (4.1)	17.5 (0.6)
	Strength (MPa)	661 (33)	629 (49)	235 (18)
TT	Modulus (GPa)	46.3 (0.8)	-	15.9 (0.3)
	Strength (MPa)	617 (39)	-	217 (7.8)

Table 2: Patch load per unit width

Overlap length, mm	Average failure load per unit width, N/mm (Std. Dev.)
25	388 (38)
50	656 (109)
75	719 (64)
120	743 (4)

Table 3: Summary of the I-beam test

Specimen	Description	Failure load, kN	Failure mode
I-beam	Steel I-beam only	96.33	Yielding of steel followed by lateral buckling
Crack	Beam with crack	99.58	Yielding of steel followed by lateral buckling
80%	Beam with 80% corrosion	104.87	Yielding followed by lateral buckling and CFRP debonding

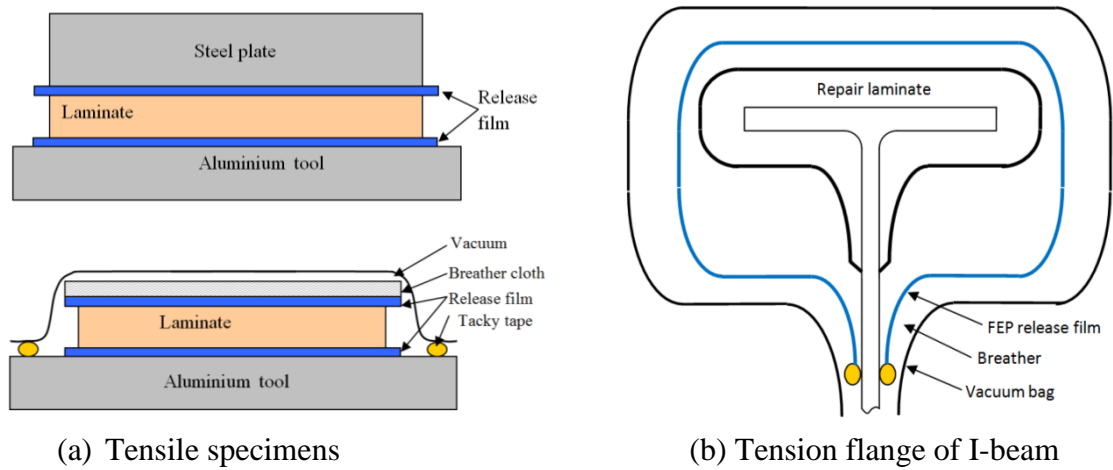
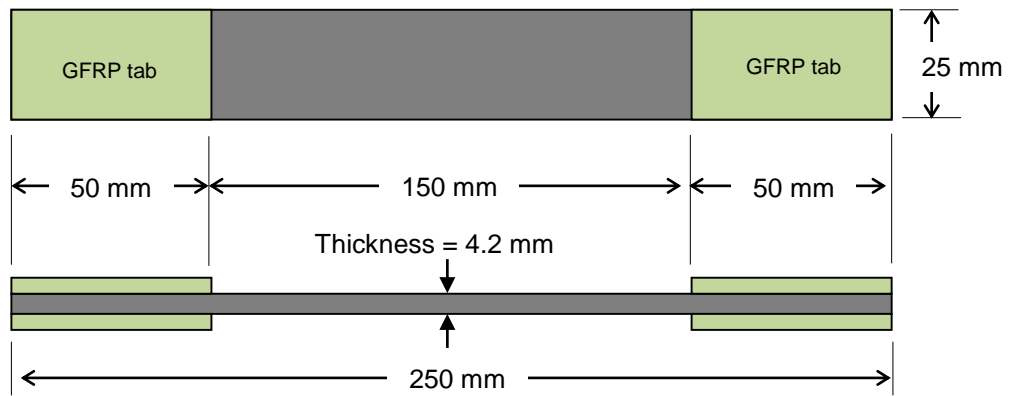
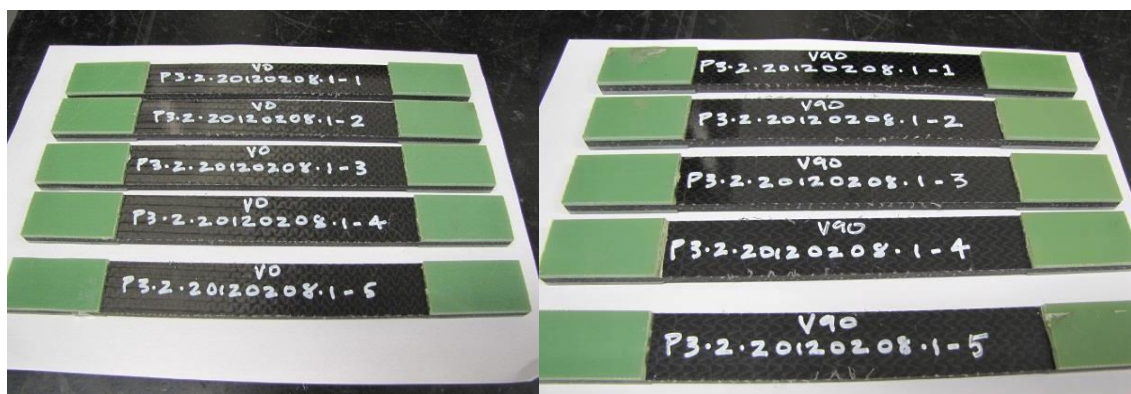


Figure 1: Consolidating of test specimens



(a) Dimensions



(b) Vacuum – LT

(c) Vacuum - TT

Figure 2: Tensile specimens

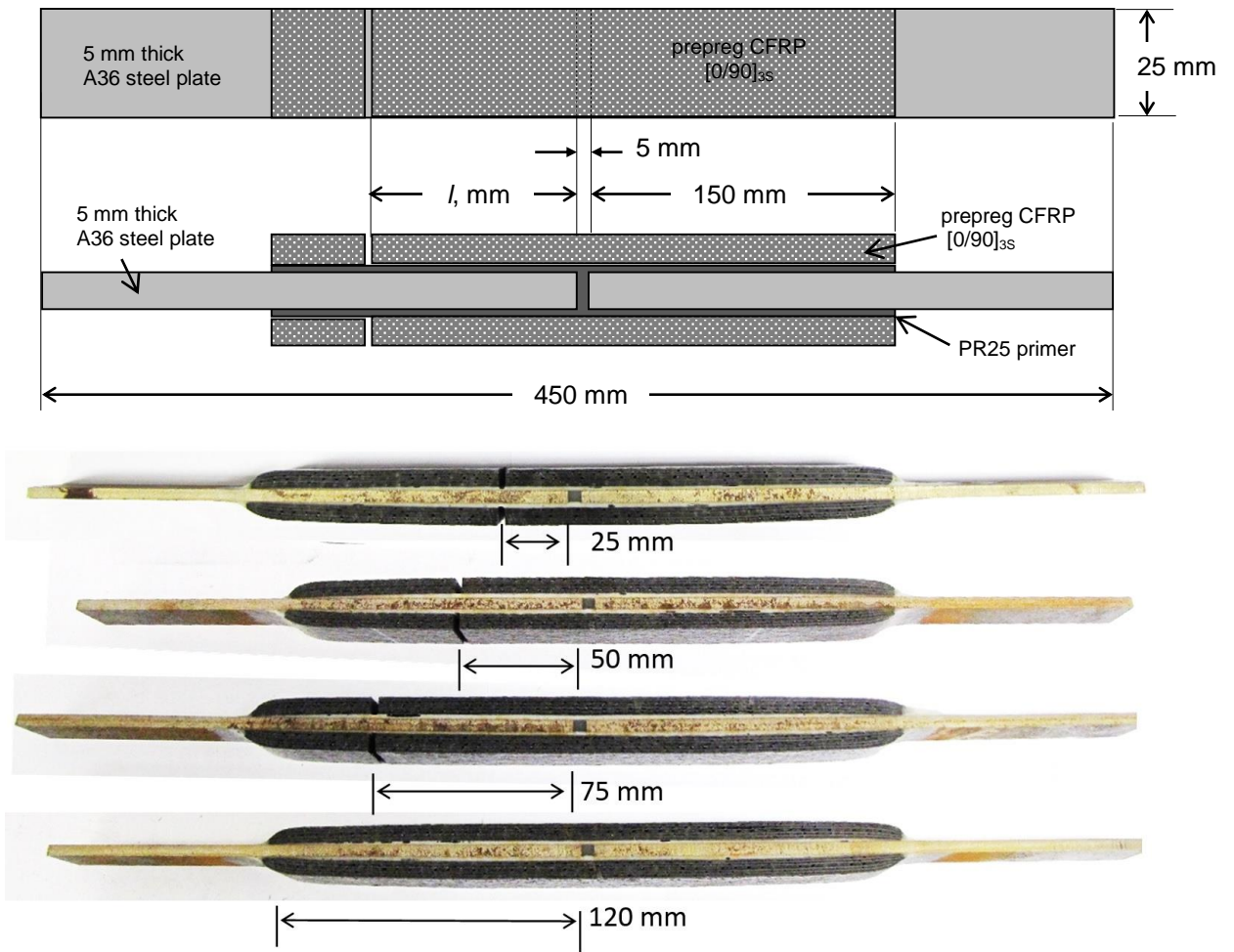


Figure 3: Double strap shear specimens with different overlap lengths

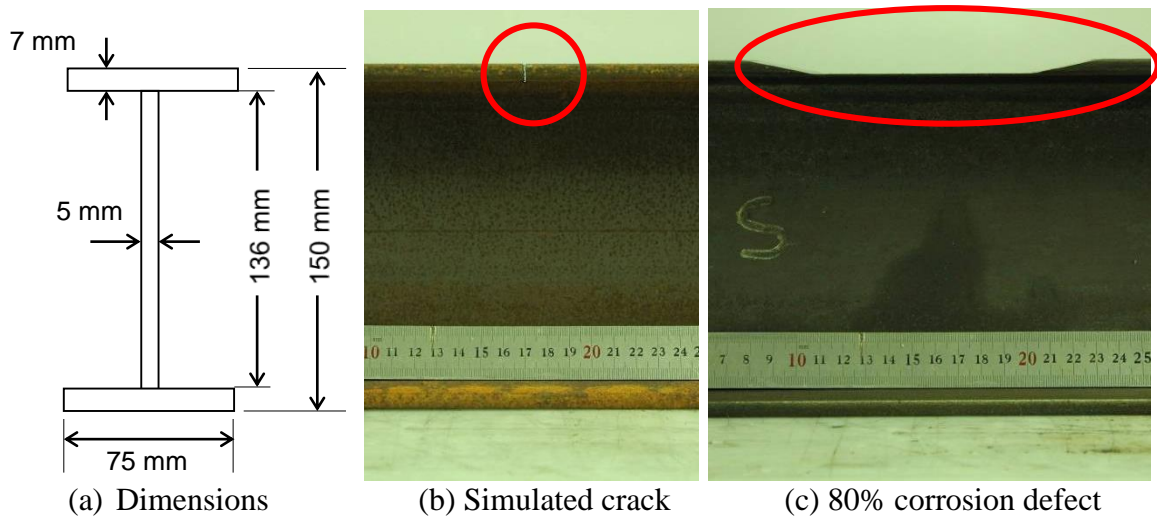


Figure 4: Details of steel I-beam specimens

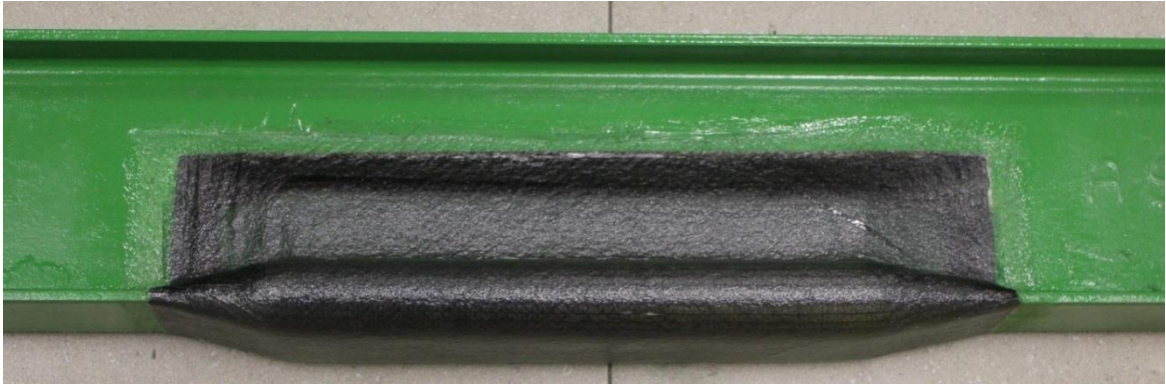


Figure 5: Patch repaired beam with simulated crack



Figure 6: Patch repaired beam with simulated 80% corrosion defect

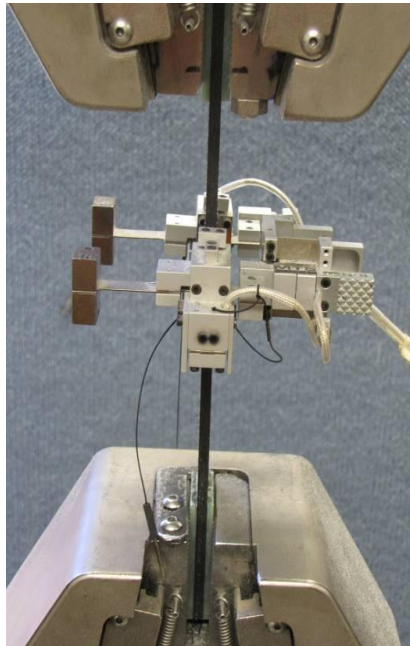


Figure 7: Setup for tensile (left) and double strap shear joint (right) tests

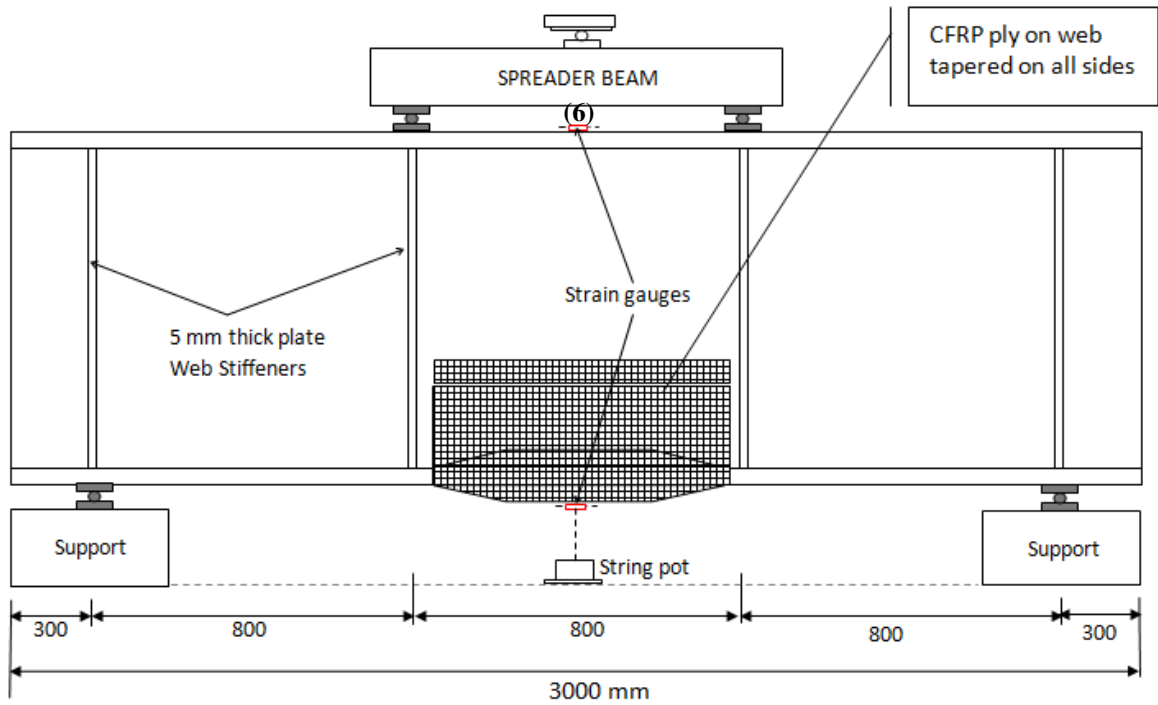
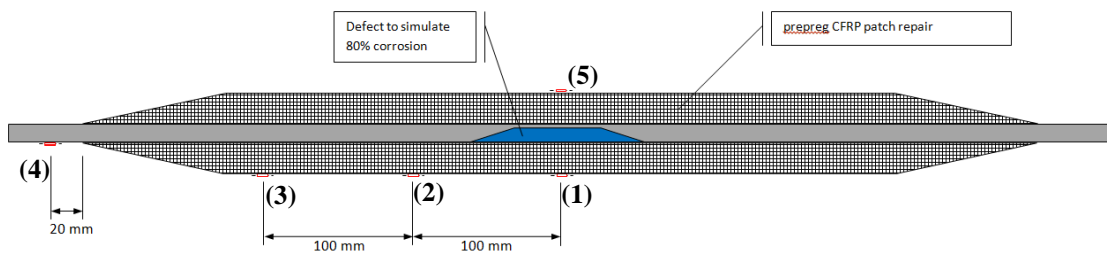
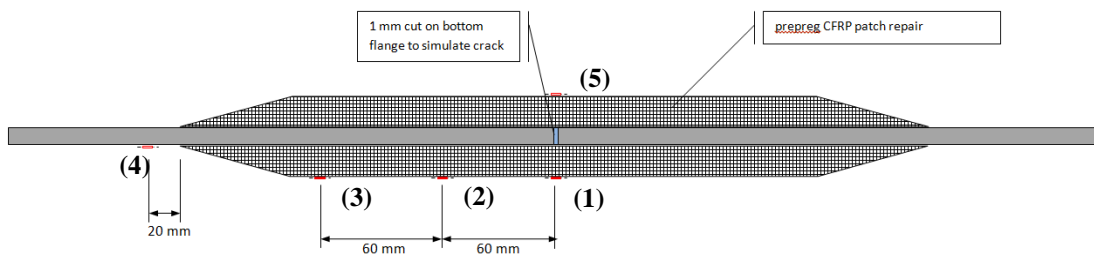


Figure 8: Static bending test set-up of Beam with simulated defects

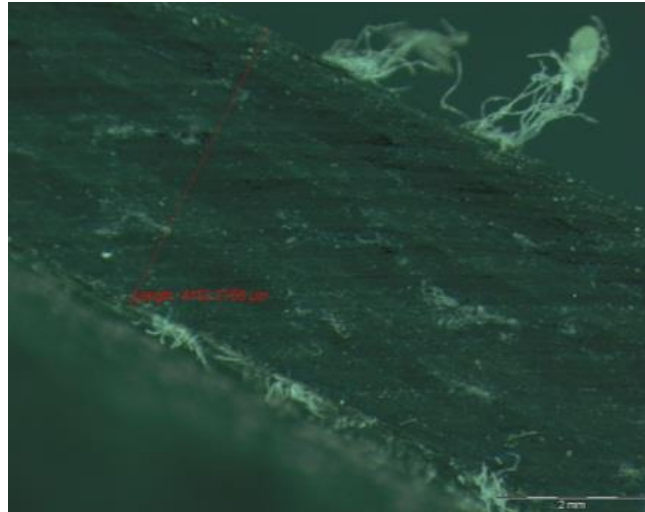


(a) Beam with simulated 80% corrosion defect

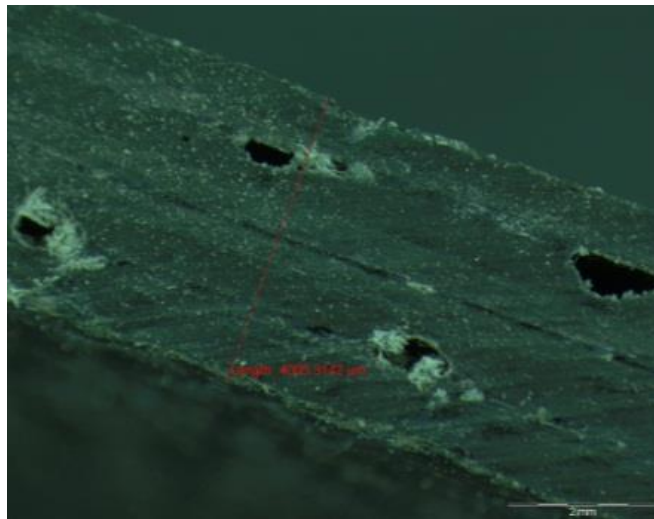


(b) Beam with simulated crack

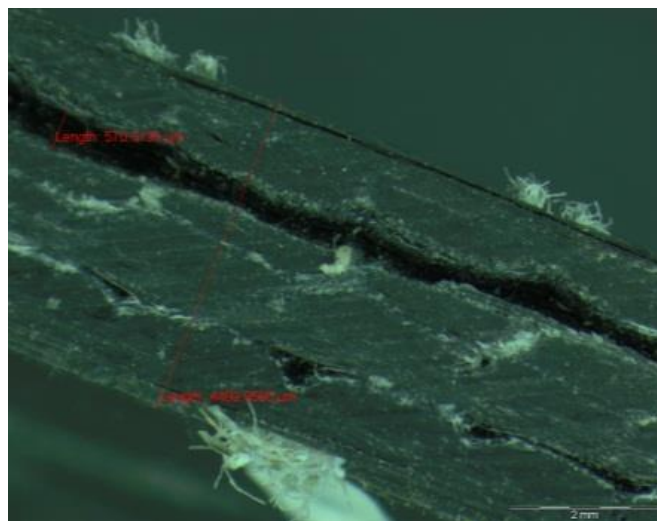
Figure 9: Location of strain gauges on the tension flange of beams



(a) Vacuum - LT

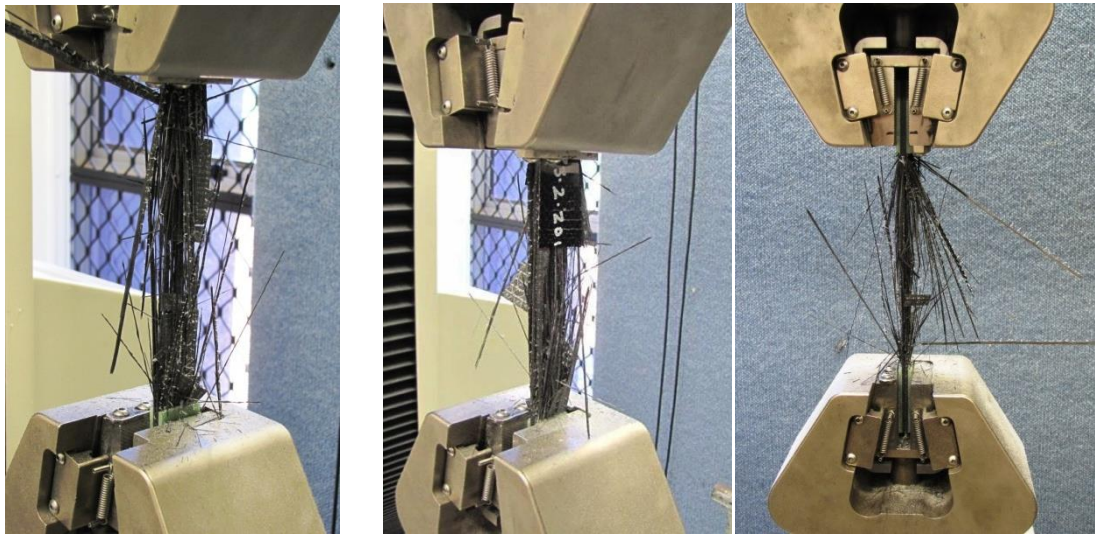


(b) Vacuum - TT



(c) No vacuum - LT

Figure 10: Microscopic observation of the tensile specimens



(a) Vacuum - LT

(b) Vacuum - TT

(c) No vacuum - LT

Figure 11: Typical failure of tensile coupon specimens

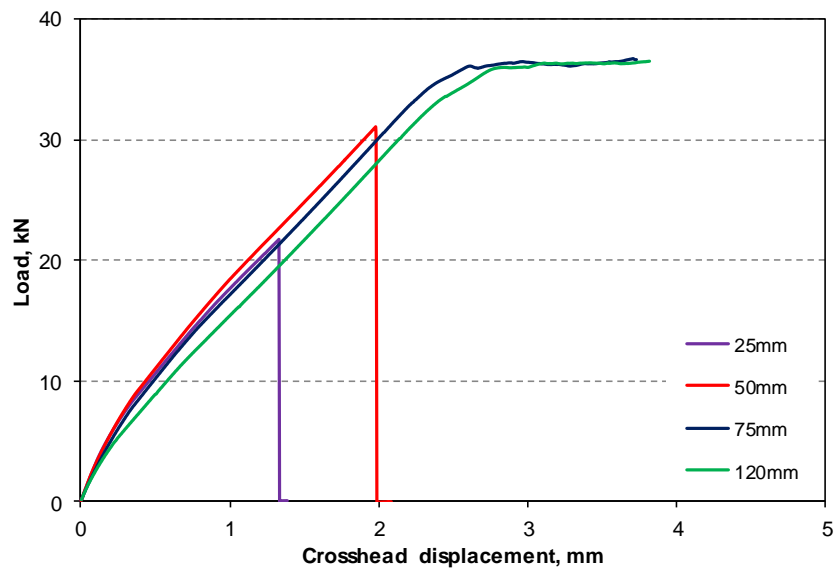


Figure 12: Load and crosshead displacement behaviour

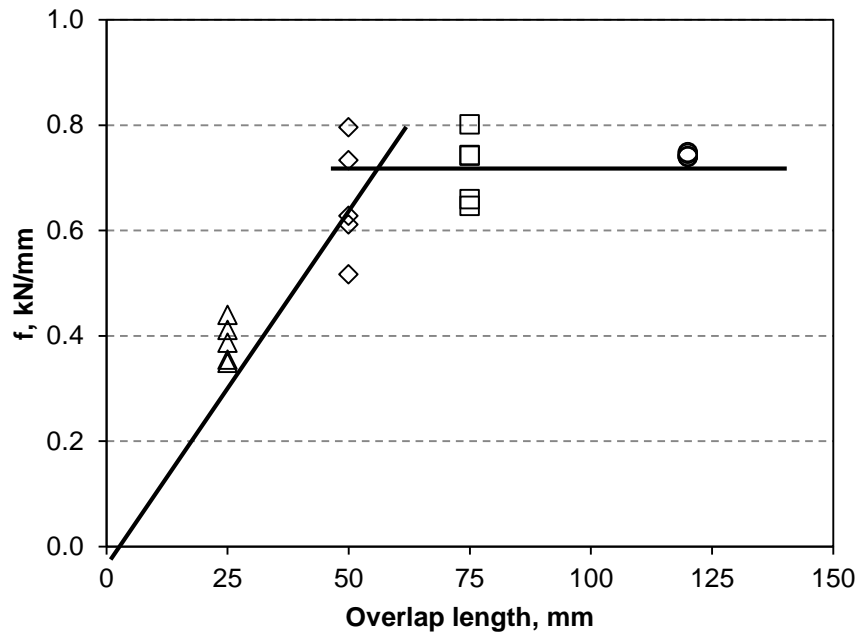


Figure 13: Relationship of patch load per unit width and overlap length

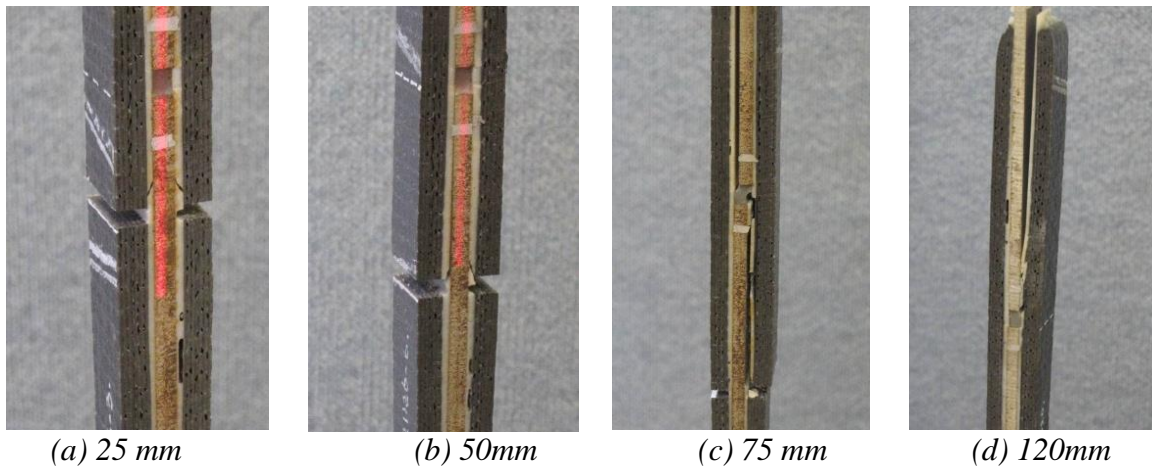


Figure 14: Typical failure of double strap shear joint specimens

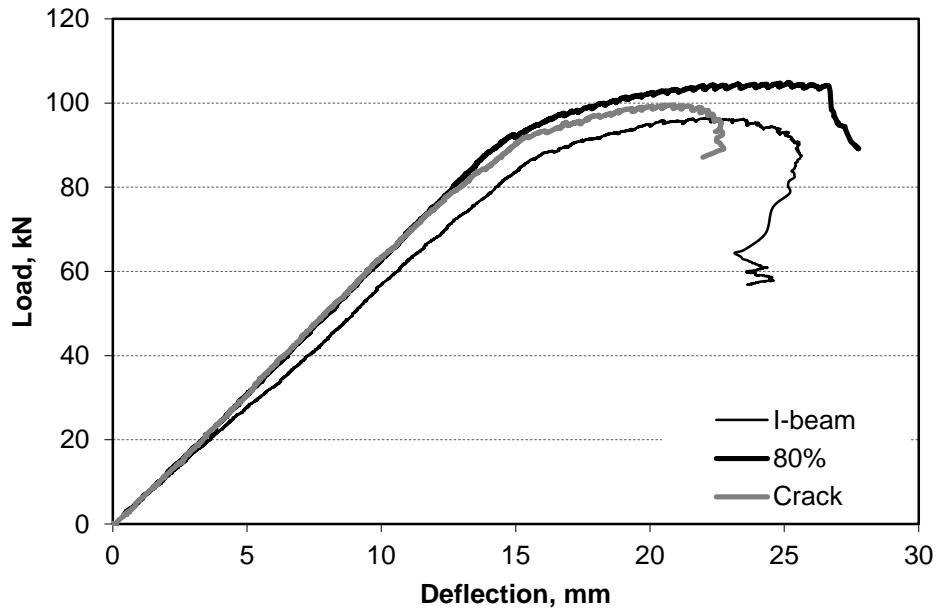


Figure 15: Load and deflection behaviour of the steel I-beams

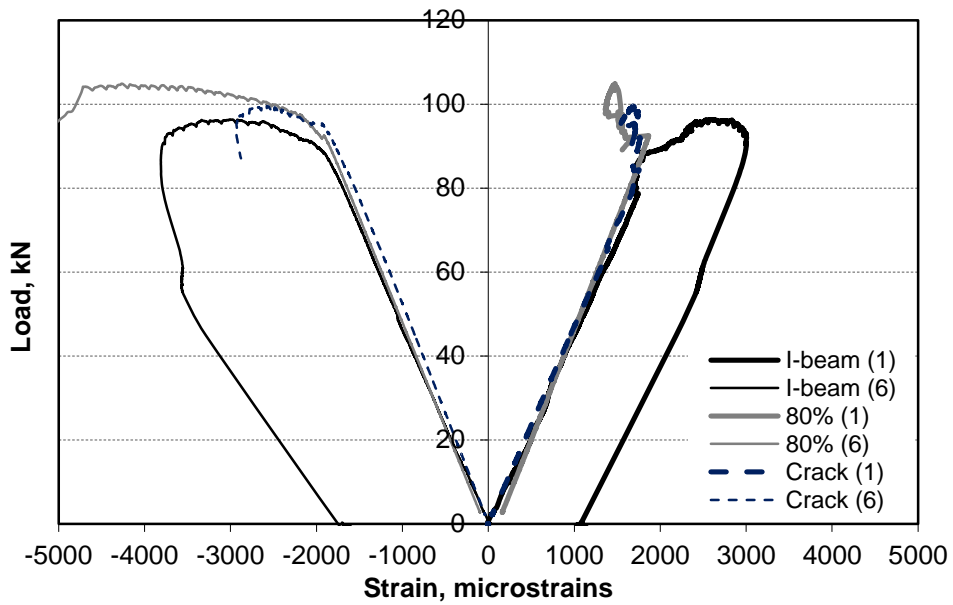


Figure 16: Load vs. strain at the top and bottom surfaces of the beams

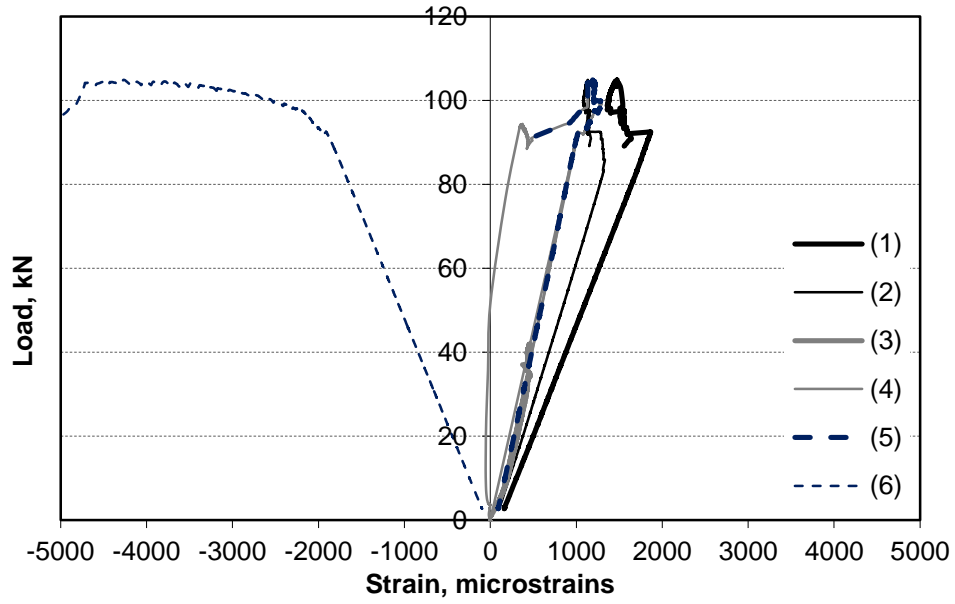


Figure 17: Load and strain relationship of the beam with 80% corrosion defect

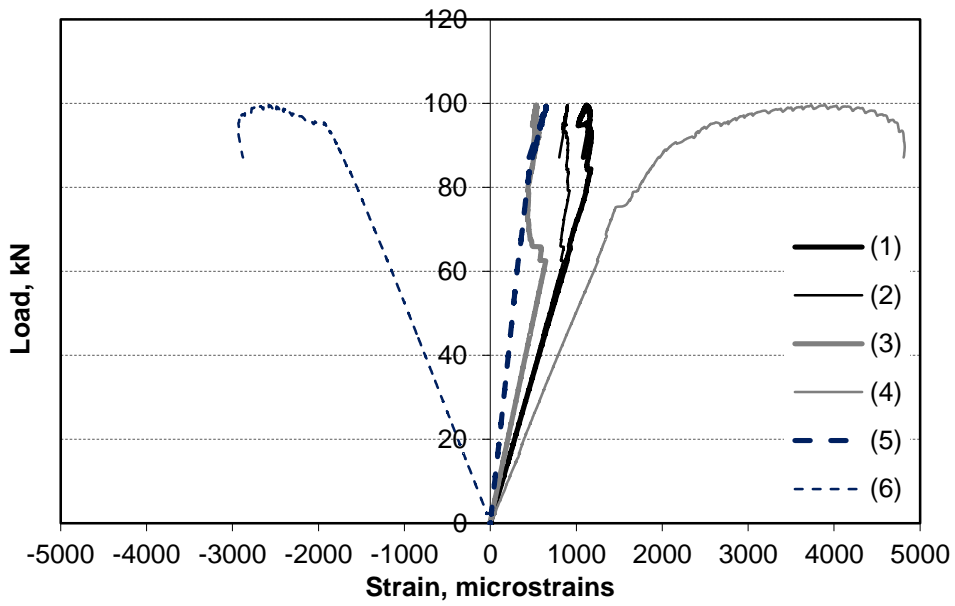


Figure 18: Load and strain relationship of the beam with crack defect

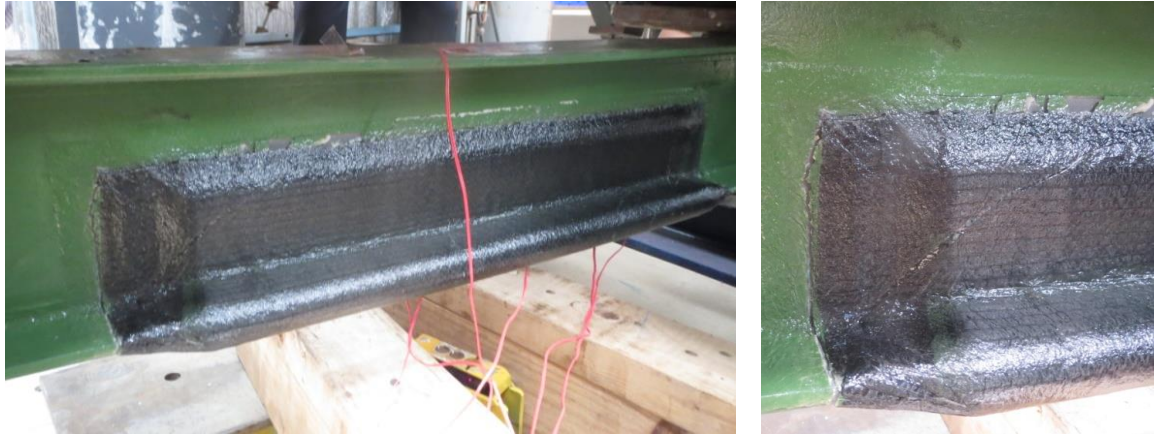


Figure 19: Disbonded patch repair to the I-beam with 80% corrosion defect

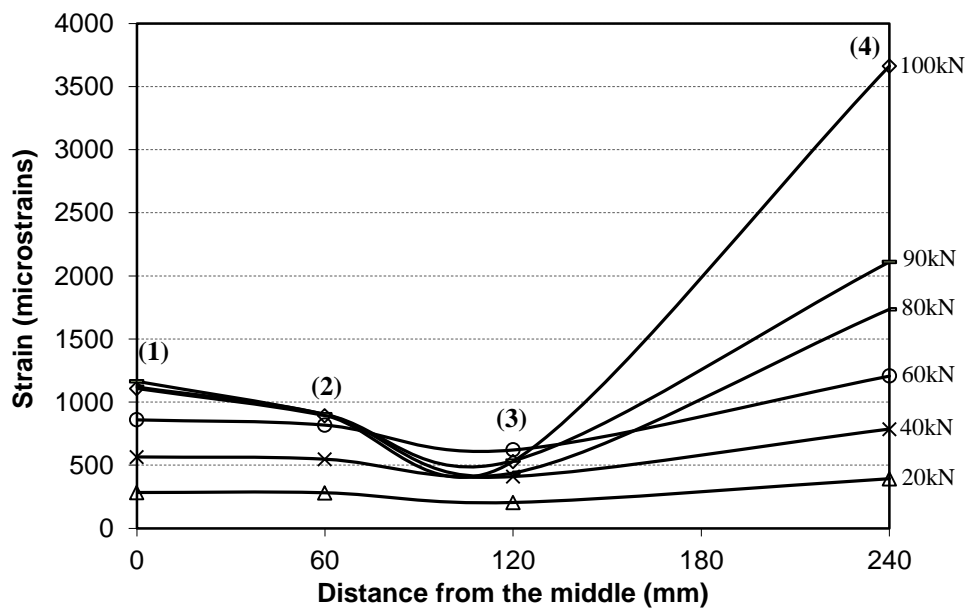


Figure 20: Load and strain relationship of the beam with crack defect

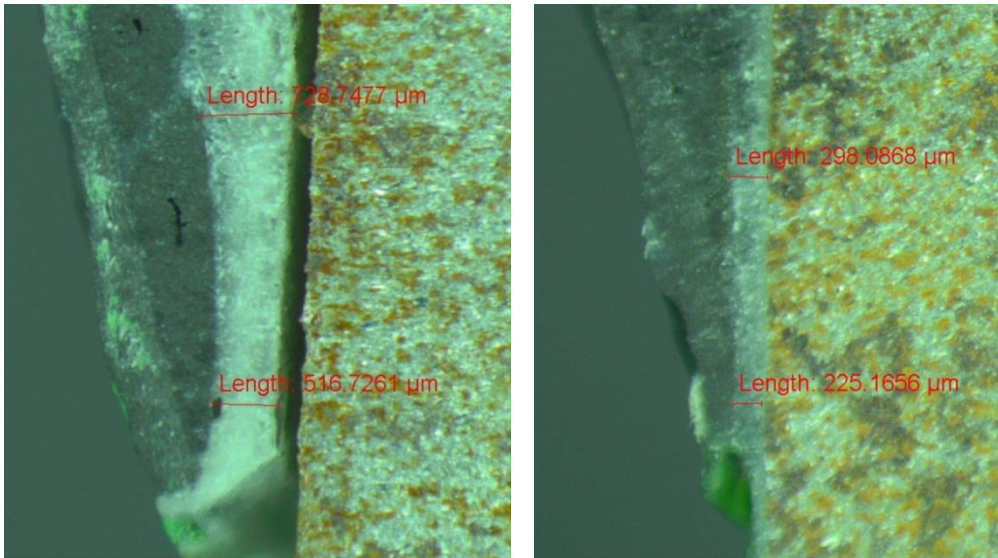


Figure 21: Microscopic observation of the end of patch repair (80% corrosion – left and crack defect – right)

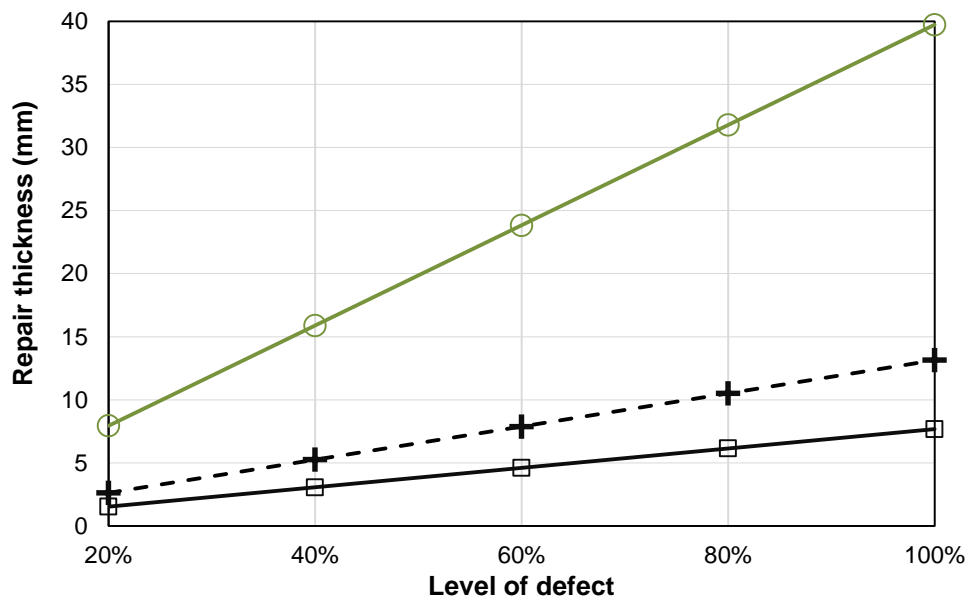


Figure 22: Required patch repair thickness for different levels of defects